J Electr Eng Technol.2018; 13(6): 2376-2384
http://doi.org/10.5370/JEET.2018.13.6.2376

ISSN(Print) 1975-0102
ISSN(Online) 2093-7423

Resonance Suppression using Sensorless Control of Dual SPMSMs Fed by Single Inverter

Jae-Boo Eom* and Jong-Woo Choi†

Abstract – To reduce the size and cost of motor driving systems, several methods for driving multiple parallel-connected motors with a single inverter have been proposed. However, dual PMSMs driven by a single inverter, unlike induction motors, have a problem with instability due to system resonance caused by disturbances such as load imbalance and tolerances between two motors. To drive dual SPMSMs fed by a single inverter, this paper proposes an active damping algorithm to effectively suppress resonance by using one-sided sensorless speed control and position difference estimation. By deriving rotor position difference from d-q current differences between two motors, the proposed method is affected less by position difference estimation errors and is simpler than dual sensorless position estimation.

Keywords: Dual SPMSMs, SIDM, Active damping control, Sensorless speed control.

1. Introduction

In general, motors fed by inverters have been widely used in industrial applications due to their system efficiency for variable loads. Although an inverter gives the benefit of efficient system control, the cost of power devices still makes up a large portion of the system cost. To reduce the system cost and size, driving parallel connected motors with single inverter has been proposed in special applications such as electric railways, steel processing, and large capacity air-conditioners.

For dual parallel-connected motors fed by a single inverter, induction motors have been widely used due to their rotor slip stability [1-7]. However, this concept has not been widely extended to PMSMs due to instability problems caused by the resonance between two motors. Various methods of multiple PMSMs drive systems have been proposed to solve this problem [8-12]. In [8] and [9], a control strategy based on the motor with the higher load to stabilize a load imbalance was proposed. In [10], dynamic stability was analyzed and the effect of motor parameters on stability was discussed. To eliminate a position sensor, a dual sensorless algorithm and stabilizing control with d-axis current of the master motor was introduced [11, 12]. In [11], an active damping control strategy based on linearization of the cosecant function was proposed. In [12], the difference between d-axis currents of each motor is used for stabilization. However, the proposed damping method in [11] is complicated to attain, and stabilization is strongly affected by master motor selection in the case of the strategy proposed in [12]. Moreover, because stabilization control is based on the difference in position between the two motors, the doubled position estimation error caused by the dual sensorless algorithm may cause performance deterioration.

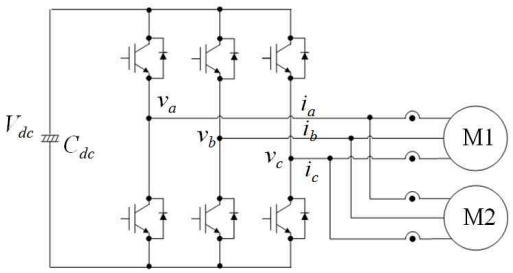

Fig. 1. Single Inverter Dual-Motor (SIDM) system

This paper proposes a simple active-damping algorithm to suppress resonance effectively by using a single sensorless speed control based on the master motor and current difference between the two motors. By deriving rotor position difference from d-q current differences between two motors, the proposed method is less affected by position difference estimation error and is simpler than dual sensorless position estimation.

2. System Analysis

2.1 Analytical model of SPMSM

Assuming the specifications of parallel-connected dual SPMSMs are the same and the speed ripple is negligible compared to the average speed, two motors in steady state can be simply modeled in the synchronous reference frame

† Corresponding Author: Dep. of Electrical Engineering, Kyungpook National University, Korea. (cjw@knu.ac.kr)
* Dep. of Electrical Engineering, Kyungpook National University, Korea. (jaeboo.eom@lge.com)
Received: April 30, 2018; Accepted: August 9, 2018

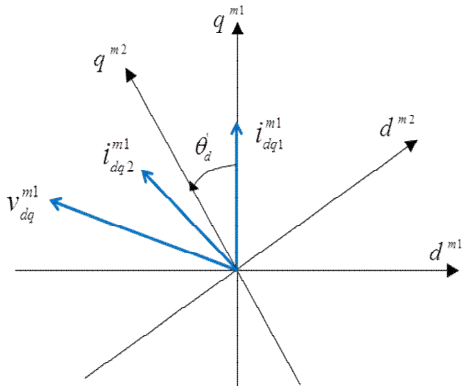

Fig. 2. Definition of synchronous reference frame based on one of dual SPMSM fed by single inverter.

of motor 1 as

$$\begin{bmatrix} v_d^{m1} \\ v_q^{m1} \end{bmatrix} = \begin{bmatrix} R_s & -\omega_r L_s \\ \omega_r L_s & R_s \end{bmatrix} \begin{bmatrix} i_{d1}^{m1} \\ i_{q1}^{m1} \end{bmatrix} + \begin{bmatrix} 0 \\ \omega_r \lambda_f \end{bmatrix} = \begin{bmatrix} R_s & -\omega_r L_s \\ \omega_r L_s & R_s \end{bmatrix} \begin{bmatrix} i_{d2}^{m1} \\ i_{q2}^{m1} \end{bmatrix} + \begin{bmatrix} -\omega_r \lambda_f \sin\theta_d \\ \omega_r \lambda_f \cos\theta_d \end{bmatrix} \tag{1}$$

$$\theta_2 - \theta_1 = \theta_d \tag{2}$$

where v_d^{m1} and v_q^{m1} are the d- and q-axis voltages; i_{d1}^{m1}, i_{d2}^{m1}, i_{q1}^{m1} and i_{q2}^{m1} are the d- and q-axis currents of motor 1 and 2 in the synchronous reference frame of motor 1; R_s is the stator resistance; L_s is the phase inductance; λ_f is the flux linkage from the permanent magnet; ω_r is the electrical rotating speed; and θ_d is rotor the position difference between motor 1 and 2. From (1), the d-q current relationship of the two motors is represented as

$$\begin{aligned} i_{d2}^{m1} &= i_{d1}^{m1} + \frac{\omega_r \lambda_f}{\alpha^2}\left(R_s \sin\theta_d - \omega_r L_s \cos\theta_d + \omega_r L_s\right) \\ i_{q2}^{m1} &= i_{q1}^{m1} - \frac{\omega_r \lambda_f}{\alpha^2}\left(R_s \cos\theta_d + \omega_r L_s \sin\theta_d - R_s\right) \end{aligned} \tag{3}$$

where

$$\alpha = \sqrt{R_s^{\,2} + (\omega_r L_s)^2} \tag{4}$$

Torques of master and slave motor are expressed as

$$\begin{aligned} T_{e1} &= k_T i_{q1}^{m1} \\ T_{e2} &= k_T\left(-i_{d2}^{m1}\sin\theta_d + i_{q2}^{m1}\cos\theta_d\right) \end{aligned} \tag{5}$$

where

$$k_T = \frac{3}{2} p \lambda_f \tag{6}$$

and p denotes number of pole-pair. If θ_d is near to zero, (3) and (5) are simplified as

$$\begin{aligned} i_{d2}^{m1} &\approx i_{d1}^{m1} + \frac{R_s \omega_r \lambda_f}{\alpha^2}\theta_d \\ i_{q2}^{m1} &\approx i_{q1}^{m1} - \frac{\omega_r^2 L_s \lambda_f}{\alpha^2}\theta_d \end{aligned} \tag{7}$$

$$\begin{aligned} T_{e2} &\approx k_T\left(-i_{d2}^{m1}\theta_d + i_{q2}^{m1}\right) \\ &\approx T_{e1} - k_T\left(i_{d1}^{m1} + \frac{\omega_r^2 L_s \lambda_f}{\alpha^2} + \frac{R_s \omega_r \lambda_f}{\alpha^2}\theta_d\right)\theta_d \end{aligned} \tag{8}$$

Eq. (8) shows that torque of motor 2 can be controlled by d-axis current of motor 1 when θ_d is not zero. It also shows that torque gain is proportional to θ_d if we can ignore the second order term.

2.2 Dynamic model and stability analysis

In this section, stability of the dual parallel connected SPMSM drive system is analyzed. For general rotating system, mechanical models for each motor are expressed as

$$\begin{aligned} T_{e1} - T_{L1} &= J_1 \frac{d\omega_{m1}}{dt} + B_1 \omega_{m1} \\ T_{e2} - T_{L2} &= J_2 \frac{d\omega_{m2}}{dt} + B_2 \omega_{m2} \end{aligned} \tag{9}$$

From (9), torque differences of two systems is written as

$$\begin{aligned} &J_2 \frac{d\omega_{md}}{dt} + B_2 \omega_{md} + T_{e1} - T_{e2} \\ &= (J_1 - J_2)\frac{d\omega_{m1}}{dt} + (B_1 - B_2)\omega_{m1} + T_{L1} - T_{L2} \end{aligned} \tag{10}$$

where

$$\omega_{md} = \omega_{m2} - \omega_{m1} \tag{11}$$

Right side term of (10) can be thought as disturbance torque T_d coming from mechanical difference between two motors. Thus, by substituting (8) to T_{e2}, (10) can be rewritten as

$$\begin{aligned} &J_2 \frac{d\omega_{md}}{dt} + B_2 \omega_{md} + p k_T \left(i_{d1}^{m1} + \frac{\omega_r^2 L_s \lambda_f}{\alpha^2} + \frac{p R_s \omega_r \lambda_f}{\alpha^2}\theta_{md}\right)\theta_{md} \\ &= T_d \end{aligned} \tag{12}$$

where

$$\theta_{md} = \theta_{m2} - \theta_{m1} \tag{13}$$

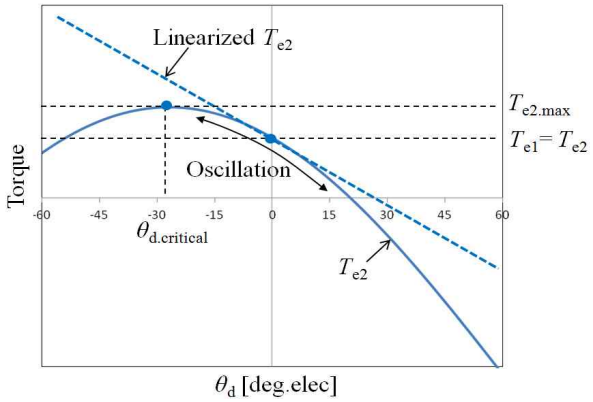

Fig. 3. Electromagnetic torque of slave motor vs. θ_d.

Fig. 3 shows that electromagnetic torque variation and oscillating behavior for θ_d of slave motor under specific speed of master motor. Assuming slave motor is oscillating at near to zero of θ_d and T_{e2} is linear for θ_d at that point, (12) can be linearized as

$$J_2 \frac{d\omega_{md}}{dt} + B_2\omega_{md} + pk_T\left(i_{d1}^{m1} + \frac{\omega_r^2 L_s \lambda_f}{\alpha^2}\right)\theta_{md} = T_d \quad (14)$$

Eq. (14) shows that the system is typical system having inertia, damper and stiffness and electromagnetic torque difference of two motors acts like stiffness. Thus, if the system doesn't have enough damping, θ_d can be amplified due to disturbance such as difference of cogging torque, torque ripple by rotor angle mismatching between two motors and load torque fluctuation. Other interesting thing is dc value of i_{d1}^{m1} also acts as additional stiffness. Because i_{d1}^{m1} can change system characteristic, i_{d1}^{m1} control in flux weakening region can make the system unstable.

For stable system, the roots of (14) should be in the left half plane of Laplace domain. So following condition should be satisfied.

$$4J_2 pk_T\left(i_{d1}^{m1} + \frac{\omega_r^2 L_s \lambda_f}{\alpha^2}\right) > 0 \quad (15)$$

As shown in (15), system stability is related with motor parameters, operating speed, inertia, damping coefficient and d- axis current of master motor. Even though (15) is satisfied, if we consider second order term of θ_d in (12), θ_d should be always larger than $\theta_{d.\text{critical}}$ to avoid operating failure of slave motor as shown in Fig. 3. Since value of $\theta_{d.\text{critical}}$ depends on motor parameter and operating speed and it moves toward zero value at lower speed, disturbance in low speed can be more critical to the system.

Fig. 4 shows actual phase currents for dual fan blower motors in air-conditioner under oscillation. Slave motor is oscillating with its natural frequency and operating failure may occur even very small disturbance.

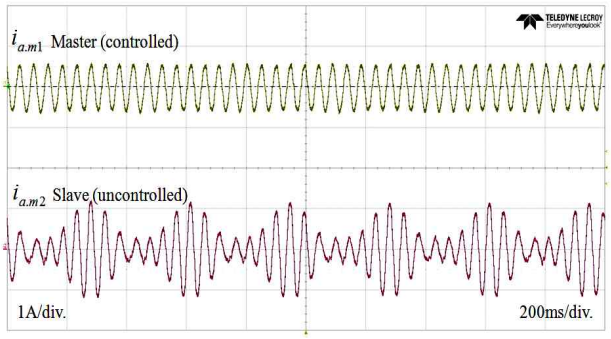

Fig. 4. Phase current oscillation of slave motor in SIDM

Since the system with very small damping coefficient can easily break down by resonance, to keep system stability independent to operating condition and system parameter, proper resonance control is needed. This can be achieved by generating additional damping torque with d-axis current of master SPMSM.

3. Resonance Suppression Control

3.1 Damping torque generation

In SPMSM, although d-axis current of master motor does not affect to torque generation of master motor, as shown in (14), it can act as an extra damping torque by controlling d-axis current as

$$T_{damp}^* = B_{eq}\omega_d = k_T\theta_d i_{d1}^{m1*}, \quad B_{eq} > 0 \quad (16)$$

By doing so, the system can be more stable with increased the system damping. From (16), d-axis current reference can be expressed as

$$i_{d1}^{m1*} = K_1\frac{\omega_d}{\theta_d}, \quad K_1 = \frac{B_{eq}}{k_T} > 0 \quad (17)$$

However, (17) is unrealizable because if θ_d is near to zero, because infinite reference d-axis current is required and dramatically changed when polarity of θ_d is changed at near to zero. Thus, proper limitation should be considered. Moreover, requiring large d-axis current compensation at very small θ_d in (17) is not effective since damping torque is proportional to θ_d as shown in (16).

The other way is to make variable damping coefficient as follows

$$B_{eq}(\theta_d) = K_2\theta_d^2 \quad (18)$$

To make the damping coefficient positive, square of θ_d is used in (18). From (16) and (18) d-axis current reference can be derived as

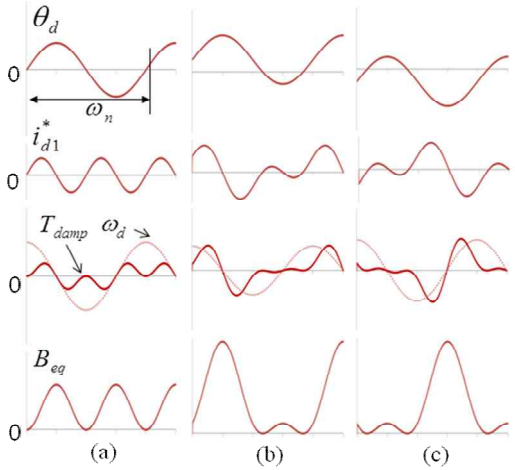

Fig. 5. Shape of damping current, torque and equivalent damping coefficient according to θ_d variation: (a) $T_{L1} = T_{L2}$, (b) $T_{L1} > T_{L2}$, (c) $T_{L1} < T_{L2}$

$$i_{d1}^{m1*} = \frac{K_2}{k_T}\theta_d \omega_d \tag{19}$$

Using (19), reference d-axis current can be very easily calculated by multiplying θ_d and ω_d. Fig. 5 shows shape of reference i_{d1}, T_{damp} and equivalent damping coefficient when θ_d is assumed as unit sine wave. It is remarkable that dc component of θ_d makes additional damping torque due to polarity of dc value when load torques are different between two motors. As result, maximum damping torque generating point is shifted.

3.2 Position and speed difference estimation

For active damping using (19), accurate phase estimating of θ_d and ω_d is important to make proper damping effect. However, using sensorless control, position estimation error is inevitable and if dual sensorless control is adopted for each motor 1 and motor 2, θ_d estimation error may be doubled. To reduce θ_d estimation error, this paper proposes driving only master by sensorless algorithm, and estimating θ_d and ω_d with only d-q current difference between master and slave motor based on master reference frame.

To derive relationship between motor current and θ_d, d, q currents of two motors, (3) can be rewritten as

$$\begin{aligned} R_s\left(i_{d2}^{m1} - i_{d1}^{m1}\right) &= \frac{\omega_r \lambda_f}{\alpha^2}\left(R_s^2 \sin\theta_d - R_s \omega_r L_s \cos\theta_d + R_s \omega_r L_s\right) \\ \omega_r L_s\left(i_{q2}^{m1} - i_{q1}^{m1}\right) &= \frac{\omega_r \lambda_f}{\alpha^2}\left(-R_s \omega_r L_s \cos\theta_d - \omega_r^2 L_s^2 \sin\theta_d + R_s \omega_r L_s\right) \end{aligned} \tag{20}$$

From (20), θ_d is estimated as

$$\hat{\theta}_d = \arcsin\left[\frac{R_s\left(i_{d2}^{m1} - i_{d1}^{m1}\right) - \omega_r L_s\left(i_{q2}^{m1} - i_{q1}^{m1}\right)}{\omega_r \lambda_f}\right] \tag{21}$$

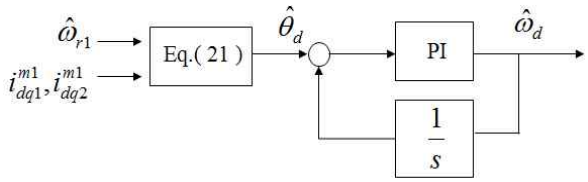

Fig. 6. Block diagram of estimating θ_d and ω_d

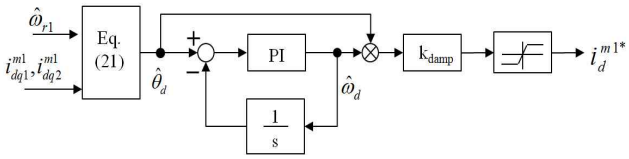

Fig. 7. Proposed reference d-axis current generation for damping control of SIDM

By using (21), proposed method has less θ_d error than getting θ_d from dual sensorless algorithm and reduces CPU calculation time.

To get ω_d, integrator and PI controller are used as Fig. 6 instead of differentiating θ_d to avoid noise caused by differentiating.

3.3 Active damping control strategy

To generate additional damping torque and stabilize the system for the disturbance torque, proposed reference d-axis current of master motor can be achieved from (19) and (21).

$$i_{d1}^{m1*} = k_{damp}\hat{\theta}_d \hat{\omega}_d \tag{22}$$

where, k_{damp} is damping gain to get a proper damping torque for the system stabilization. As known in (22), proposed method is operated only with current difference between two motors. Therefore, the proposed method does not need to calculate θ_d or ω_d from speed and position of each motor, and it can operate with only one position sensor or position sensorless control of master motor.

Fig. 7 shows block diagram of proposed reference d-axis current generation method of master motor for damping control without measuring or estimating θ_d and ω_d.

4. Experimental Evaluation

4.1 Simulation

Fig. 8 and Table 1 show a total control system block diagram and motor specifications for simulation. In the simulation, the current model based back-EMF estimator is used as sensorless speed control algorithm [13, 14]. The speed estimation and control is performed based only motor 1 (master motor) and d, q axis currents of slave motor are expressed as reference frame of master motor. Speed and angle oscillation of slave motor are estimated by

Table 1. Nominal parameters for 900 W SPMSM

Base Speed	1000 rpm
R_s	7.5 Ω
L_s	60 mH
Rated Torque	0.062 Nm
λ_f	0.413 Wb
Number of poles	8

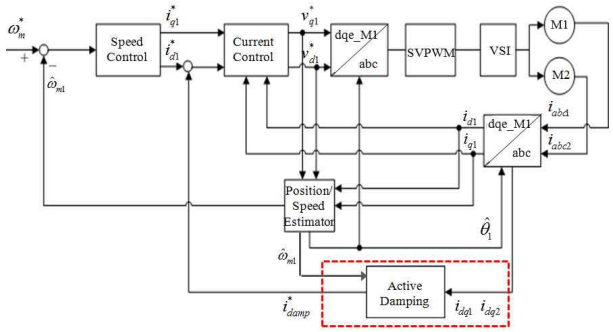

Fig. 8. Proposed control block diagram for SIDM system

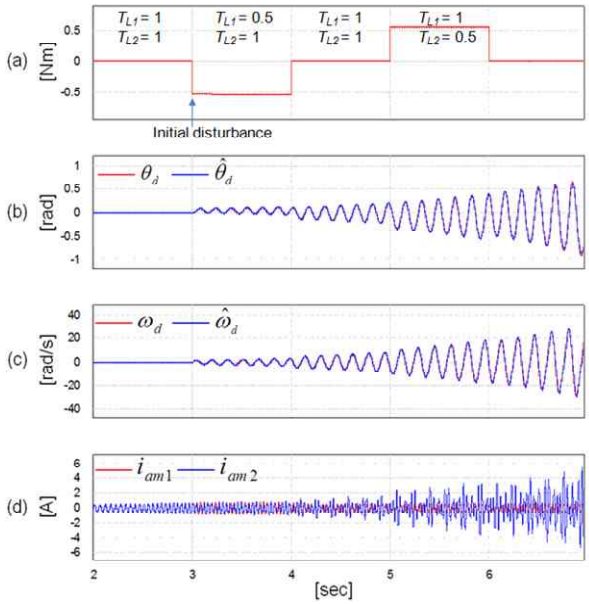

Fig. 9. Simulation result of estimating θ_d and ω_d with proposed method without damping control: (a) $T_{L1}-T_{L2}$, (b) θ_d and estimated θ_d, (c) ω_d and estimated ω_d, (d) Phase current of master and slave motor

(21) and Fig. 6. To generate extra damping torque to suppress the oscillation of slave motor, (22) is used for reference d-axis current of master motor.

Fig. 9 shows the simulation result of estimated transient angle and speed difference between two motors that is not considered damping torque when various instantaneous load unbalances. Initially, speed of two motors is 400 rpm with constant load of 1 Nm for 3 second in steady state. After then, sudden loads changes of 0.5 Nm are applied to each motor for every second. Since initial disturbance

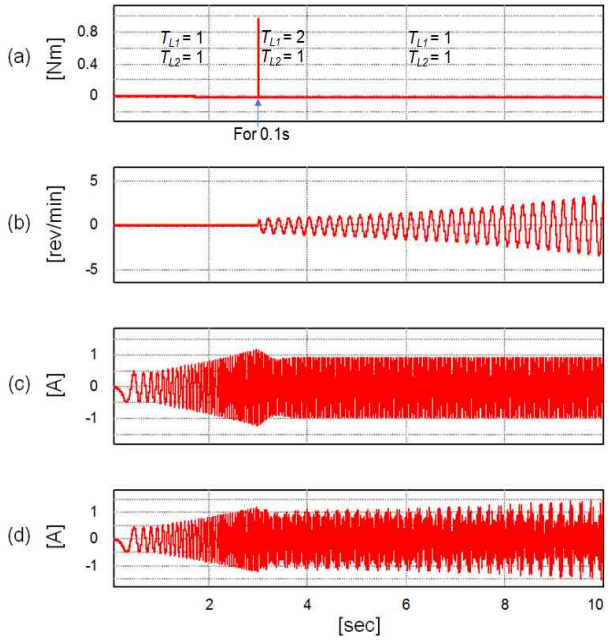

Fig. 10. SIDM system responses of master motor based speed control without damping control: (a) Load torque difference between master and slave($T_{L1}-T_{L2}$), (b) Speed difference, ω_d, (c) Phase current of master motor, (d) Phase current of slave motor

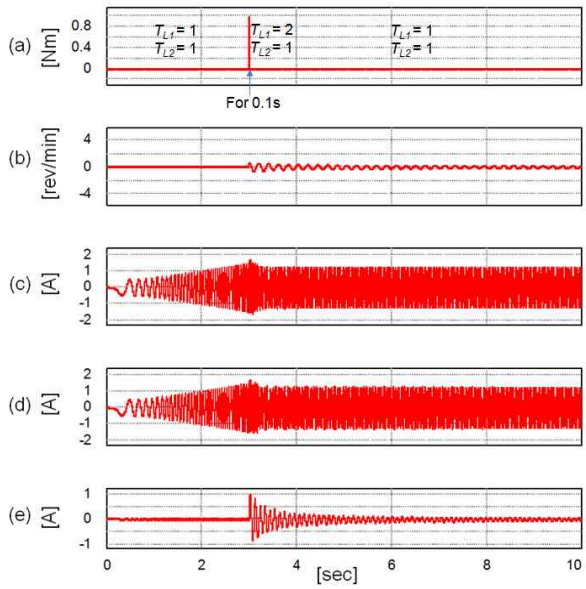

Fig. 11. SIDM system responses of master motor based speed control with proposed damping control: (a) Load torque difference between master and slave ($T_{L1}-T_{L2}$), (b) Speed difference, ω_d, (c) Phase current of master motor, (d) Phase current of slave motor, (e) d-axis current of master motor

is applied for 3 second, system response can be observed after 3 second as shown in Fig. 9 (b) and (c). From these results, it is verified that (21) is reasonable even though slave motor is very unstable and not affected by

instantaneous torque variation between two motors. It is noted that proposed estimation method may have amplitude error due to parameters change such as temperature effect. However, it is not important because phase error is more important to generate proper damping torque corresponding oscillating status. Moreover, proposed method has less phase error because the algorithm is based on the measured currents.

Fig. 10 and 11 show simulation results of SIDM system, which is based on master motor with/without proposed damping control when disturbance torque is applied. In the simulation, two motors are accelerated to 400 rpm for 3 second with the same load condition (1 Nm). After then, short term load of 2 Nm is applied to master motor for 0.1 second to make disturbance on the SIDM system. Fig. 10 shows that SIDM system without damping control is diverging just after disturbance is applied. In case that the proposed control method is used, system can be stabilized within several seconds as shown in Fig. 11. Fig. 12 is result of transient response of master and slave motor for load difference variation. Under the same load of 1 Nm at 400 rpm, additional 0.5 Nm is applied on master and slave motor for a second. It is remarkable that oscillation in case of unbalanced load is faster decayed than that in case of balanced load. It can be explained that more damping torque is generated when loads of two motors are different due to dc component of θ_d as shown in Fig. 5.

4.2 Experiment result

To verify the damping effect of the SIDM system by the proposed method, an experimental system was constructed with two 900W SPMSMs for dual fan blowers faced to top side of 20HP air-conditioner outdoor unit, inverter drive and measuring equipment as shown in Fig. 13. Inverter for SIDM drive was composed with 4 current sensors for sensing phase currents of each motor, 4 channels of DAC and IPM that its outputs are connected to motors in parallel. Inverter was driven by DC 520V and switching frequency was chosen as 7 kHz. As an important system characteristic, mechanical resonance frequency of the system was known

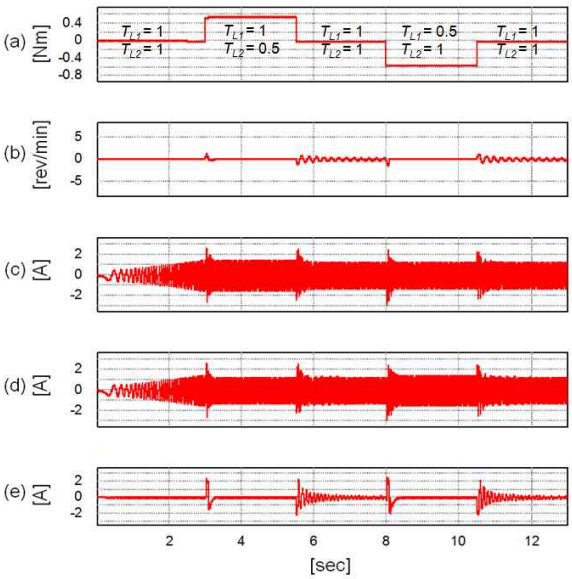

Fig. 12. SIDM system responses of master motor based speed control with proposed damping control: (a) Load torque difference between master and slave ($T_{L1} - T_{L2}$), (b) Speed difference, ω_d, (c) Phase current of master motor, (d) Phase current of slave motor, (e) d-axis current of master motor

(a) (b)

Fig. 13. Experiment construction: (a) Outdoor unit of air-conditioner, inverter drive and measurement system, (b) Dual fan blower on top-side of outdoor unit

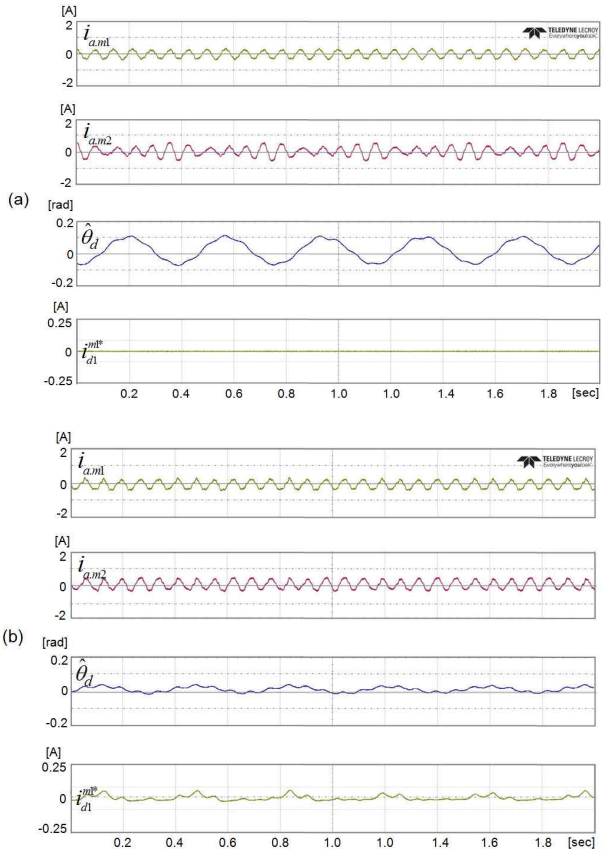

Fig. 14. Steady state operation at 200 rpm: (a) without active damping (b) proposed damping control

as speed range of 350~400 rpm from mechanical noise and vibration test.

The experiment to verify the effect of proposed damping control proceeded in the following. At first, to find unstable speed region in driving SIDM, position sensorless control based one of two motors (master motor) was performed for several steps of speed without active damping control. At this time, amplitude variation of phase current of the other motor (slave motor) was observed for each step of speed. By doing so, unstable speed range of the system can be detected. After that, phase current, estimated θ_d and ω_d were compared with/without proposed damping control in steady state. In case of the experiment system, phase current oscillation was appeared at 200~500rpm. Especially, in speed range of 350~400 rpm, SIDM driving was impossible without proper damping control due to resonance of the system at that speed range.

Fig. 14, 15 and 16 are test results in steady state operation of SIDM system for 200, 300 and 500 rpm. As shown in the Fig. 14 to 16, compared to without d-axis current control, oscillation of slave motor is dramatically improved by proposed method. It is noted that periodic oscillation is independent to the motor speed. This phenomenon can be understood as natural frequency of the SIDM system analyzed from (14). The reason that the oscillation is relative high in 300 rpm is due to increment of structural vibration caused by mechanical resonance of fan blade and structural system that is positioned at 350~400 rpm. Because the amplitude of disturbance is not always the same for oscillation period, it is shown that d-axis current is slightly different for the period.

Fig. 17 shows the performance of proposed active damping control. In the experiment, sensorless speed control

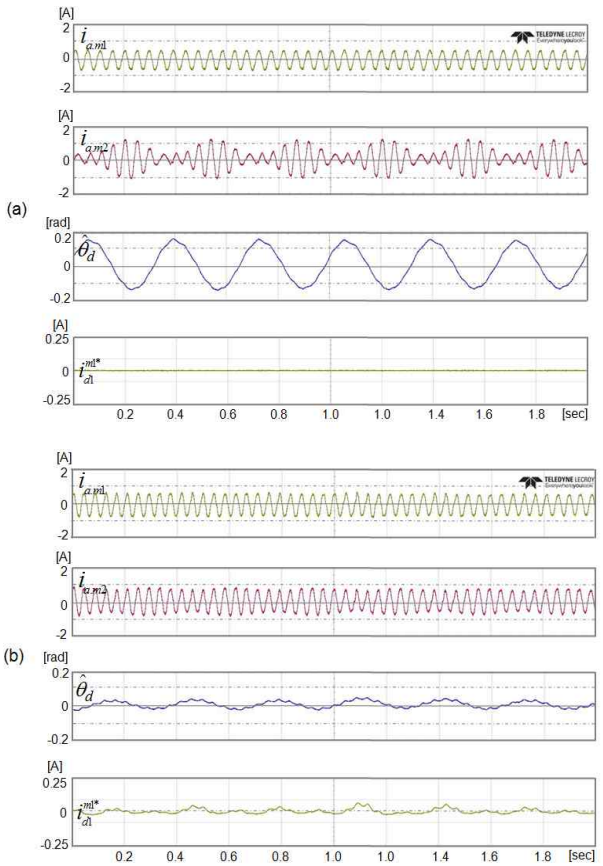

Fig. 15. Steady state operation at 200 rpm: (a) without active damping (b) proposed damping control

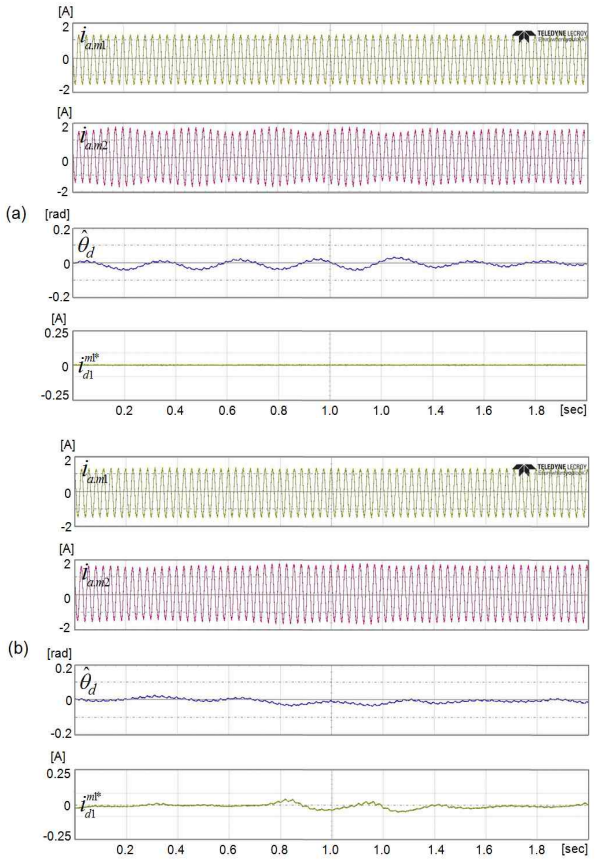

Fig. 16. Steady state operation at 500 rpm: (a) without active damping (b) proposed damping control

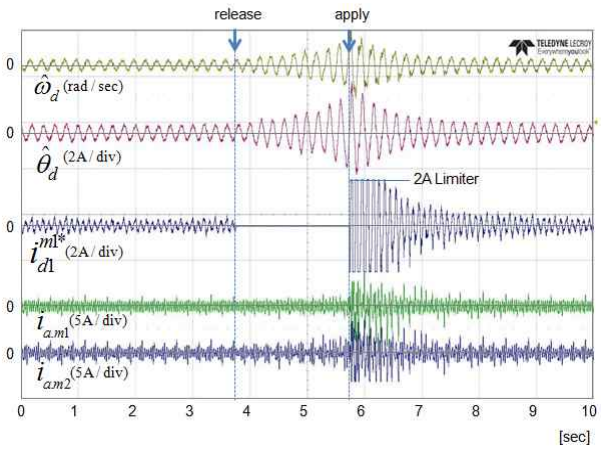

Fig. 17. Experimental waveform when the proposed damping control is released and applied at 400 rpm

based one of two motors is performed to speed up to 400 rpm with proposed damping control to avoid break down, and then the performance of proposed method is evaluated by releasing and reapplying d-axis current. Considering hardware specification, reference of d-axis current is limited to 2A. From the result, stopping the d-axis control results that system is diverging as time goes by. After several seconds, damping control is reapplied and the system is stabilized again. However, it is shown that d-axis current is compensating to stabilize under continuous disturbance even though the system is under steady state. It is explained that this system generates a disturbance continuously during operating such as electromagnetic torque ripple, cogging torque, unbalance of fan blades, inertia differences etc. Moreover, since tested speed range (400 rpm) is mechanical resonance range of the system, these disturbances amplify the oscillation of SIDM.

5. Conclusion

This paper has derived relation between rotor position difference and d-q axis current difference of dual motor, which is independent to d-q current of controlled motor in SIDM under small oscillation. Also, this paper has proposed the active damping algorithm to suppress resonance effectively based on sensorless speed control using q-axis current and damping control using d-axis current of master motor. To achieve more precision damping control, this paper proposed very simple and effective active damping torque control method based direct position differences calculation using detected current without speed or position estimation of slave motor using dual sensorless algorithm. The proposed algorithm is able to stably drive the overall load torque area and has the advantage of reduced computation because it uses only one speed controller.

Finally, it is verified that the proposed algorithm is stably operated in dual fan blower system motors connected in parallel by experiment and it can be operated stably during asynchronous load fluctuations and high frequency load change conditions via simulations with a three-phase inverter system.

References

[1] E. Levi, M. Jones and S. N. Vukosavic, "Even-phase multi-motor vector controlled drive with single inverter supply and series connection of stator windings," *IEE Pro. Electr. Power Appl.*, vol. 150.

[2] M. Jones, S. N. Vukosavic, D. Dujic, E. Levi, and P. Wright, "Five-leg inverter PWM technique for reduced switch count two-motor constant power applications," *IET Electr. Power Appl*., vol. 2, no. 5, pp. 257-287, Sep. 2008.

[3] Hyung-Woo Lee "Study on Characteristic due to Deviation of the Wheel Diameters with Parallel Operation," *Journal of Electrical Eng. & Tech.* vol. 8, no. 1, pp. 106-109, Feb. 2012.

[4] P. M. Kelecy and R. D. Lorenz, "Control methodology for single inverter, parallel connected dual induction motor drives for electric vehicles," in *Proc. IEEE Power Electron. Spec. Conf.*, 1994, vol. 2, pp. 987-991.

[5] F. Xu, L. Shi, and Y. Li, "The weighted vector control of speed-irrelevant dual induction motors fed by the single inverter," *IEEE Trans. Power Electron.*, vol. 28, no. 12, pp. 5665-5672, Dec. 2013.

[6] I. X. Bogiatzidis, A. N. Safacas, E. D. Mitronikas, and G. A. Christopoulos, "A novel control strategy applicable for a dual AC drive with common mechanical load," *IEEE Trans. Ind. Appl.*, vol. 48, no. 6, pp. 2022-2036, Nov./Dec. 2012.

[7] K. Matsuse, H. Kawai, Y. Kouno, and J. Oikawa, "Characteristics of speed sensorless vector controlled dual induction motor drive connected in parallel fed by a single inverter," *IEEE Trans. Ind. Appl.*, vol. 40, no. 1, pp. 153-161, Jan./Feb. 2004.

[8] D. Bidart, M. Pietrzak-David, P. Maussion, and M. Fadel, "Mono inverter dual parallel PMSM-Structure and Control strategy," *34th Annual Conference of IEEE. IECON 2008*, pp. 268-273, Nov. 2008.

[9] D. Bidart, M. Pietrzak-David, P. Maussion, and M. Fadel, "Mono inverter multi-parallel permanent magnet synchronous motor: structure and control strategy," *IET, Electric Power Applications*., vol. 5, no. 3, pp. 288 294, Mar. 2011.

[10] Yongjae Lee, Jung-Ik Ha, "Control Method for Mono Inverter Dual Parallel Surface Mounted Permanent Magnet Synchronous Machine Drive System," *2014 IEEE Energy Conversion Congress and Exposition (ECCE)*, pp. 4843-4849, Sept. 2014.

[11] Yongjae Lee, Jung-Ik Ha, "Control Method for Mono Inverter Dual Parallel Surface Mounted Permanent Magnet Synchronous Machine Drive System," *IEEE Transactions on Industrial Electronics.*, vol. 62, pp. 6096 - 6107, April 2015.

[12] Chang-Bum Kim, Chul Yun, Byung-Keun Yoon, Nae-Soo Cho, Woo-Hyen Kwon, "Parallel Sensorless Speed Control using Flux-axis Current for Dual SPMSMs Fed by a Single Inverter," *Journal of Electrical Engineering & Technology* vol.10 no.3,pp. 1048-1057 Mar. 2015.

[13] N. Matsui, T. Takeshita, and K. Yasuda, "A new sensorless drive of brushless DC motor," in *Proc. IECON '92*, pp. 430-435, 1992.

[14] N. Matsui, "Sensorless PM brushless DC motor drives," *IEEE Trans. Ind. Electron*., vol. 43, no. 2, pp. 300-308, Apr. 1996.

Jae-Boo Eom He received B.S degree in mechanical engineering from Pusan National University, Busan, Korea, in 1999, and M.S. degree in mechanical engineering, Pusan National University, Pusan, Korea, in 2001 and currently a Ph.D course student in electrical engineering with School of Electronics Engineering, Kyungpook National University (KNU), and work for LG electronics Inc simultaneously. His research interests are electric machinery, motor control and power electronics.

Jong-Woo Choi He received the B.S., M.S., and Ph.D. degree in electrical engineering from the Seoul National University, Seoul, Korea, in 1991, 1993, and 1996, respectively. From 1996 to 2000, He worked as a Research Engineer at the LG Industrial Systems Company, Korea. Since 2001, he has been a Professor in the Department of Electrical Engineering at Kyungpook National University, Daegu, Korea. His current research interests include static power conversion and electric machine drives.